

Research Paper

# Deep Learning- Model Predictive Control for Load Frequency Control of Microgrids with Electric Vehicles

Farhad Amiri <sup>\*</sup> , and Sajad Sadr 

Department of Electrical Engineering, Tafresh University, Tafresh 39518-79611, Iran.

**Abstract**— In an islanded microgrid, ensuring frequency stability is essential for reliable system operation. Distributed generation (DG) and electric vehicles (EVs) make frequency stability challenging in an islanded microgrid because they increase generation and load variability and reduce system inertia. Load frequency control (LFC) is mainly used to enhance the frequency response of these types of microgrids. In addition, uncertainty in parameters and perturbations strongly impact the application of LFC. To address these challenges, this paper presents an LFC method for islanded microgrids using model predictive control (MPC) based on deep learning. The deep learning technique is used to enhance MPC controller performance against uncertainties and disturbances. The proposed method is validated through experiments, especially in the presence of disturbances and parameter instability. It is then compared with other methods, including linear active disturbance rejection control (LADRC), fractional-order PID (FOPID), and several others. The results show that the MPC method based on deep learning outperforms these approaches in terms of disturbance rejection, frequency response improvement, and system inertia enhancement.

**Keywords**—Deep learning, electric vehicle, islanded microgrid, load frequency control.

## NOMENCLATURE

### Abbreviations

CCSA	Chaotic Crow Search Algorithm
COA	Coati Optimization Algorithm
ESS	Energy Storage System
FNN	Feedforward Neural Network
GWO	Grey Wolf Optimization
SG	Synchronous Generator
SMC	Sliding Mode Control
SO	Sailfish Optimizer
SSO	Salp Swarm Optimization

### Parameters and Variables

$\beta$	Frequency bias factor
$\Delta f$	Frequency variation
$\Delta P_{ESS}$	Energy Storage System (ESS) power variation
$\Delta P_{FC}$	Fuel Cell (FC) power variation
$\Delta P_g$	Generator output power variation
$D$	Load-damping factor
$F_p$	Fraction of total turbine power
$FR$	Frequency response
$K_{ESS}$	ESS gain
$K_{EV}$	EV battery gain
$K_{FC}$	FC gain
$K_{PV}$	PV gain

$K_{WT}$	WT gain
$M$	Inertia constant
$R$	Speed regulation
$T_c$	Turbine time constant
$T_g$	Governor time constant
$T_r$	Reheat time constant
$T_{ESS}$	ESS time constant
$T_{EV}$	EV battery time constant
$T_{FC}$	FC time constant
$T_{PV}$	PV panel time constant
$T_{WT}$	WT time constant

## 1. INTRODUCTION

The presence of DGs and EVs in the power system has been one of the fundamental and impactful transformations in the structure of power systems in recent decades [1]. These technologies have not only changed the way energy is produced and consumed but have also created new challenges and opportunities in the areas of sustainability, efficiency, and power system management [2]. DGs refer to small electricity generation units that are directly connected to power systems and, unlike traditional centralized power plants, are located close to consumers [3]. These resources include Photovoltaics (PVs), Wind turbines (WTs), Fuel cells (FCs), and small thermal power plants [4]. As the generation of electricity from renewable sources continues to expand and the demand to lower greenhouse gas emissions grows, the adoption of the DG system has increased [5]. The presence of DGs in power systems offers multiple advantages, including reduced transmission losses, increased system stability, decreased dependence on fossil fuels, and improved energy security [6]. However, these resources also bring challenges. Among these challenges are the fluctuations in electricity production from renewable sources like wind and solar, the need for smart energy management, and the lack of full compatibility with the traditional structure of power systems [7].

Received: 14 Nov. 2024

Revised: 11 Jan. 2025

Accepted: 12 Feb. 2025

\*Corresponding author:

E-mail: f.amiri@tafreshu.ac.ir (F. Amiri)

DOI: 10.22098/joape.2025.16193.2250

This work is licensed under a [Creative Commons Attribution-NonCommercial 4.0 International License](https://creativecommons.org/licenses/by-nc/4.0/).

Copyright © 2025 University of Mohaghegh Ardabili.

The presence of EVs is increasingly recognized as an important component of the power system. EVs not only serve as consumers of electricity for the grid but can also function as sources of energy production or storage using technologies like Vehicle to Grid (V2G). During charging, these vehicles draw power from the grid, and during peak demand periods, they can return stored energy back to the grid [8]. A microgrid is a small, independent network from the power system that can operate connected to the main grid or in an island mode. Control of the microgrid in islanded mode must effectively manage its local generation and consumption [9]. One of the fundamental issues in islanded microgrids is frequency stability, which is managed through Primary control (PCs) and LFC systems. When a disturbance happens, the power controllers manage frequency fluctuations but cannot bring the frequency back to its nominal value; this function is performed by the LFC system using different controllers [10].

The presence of DGs and EVs poses challenges to the LFC system, such as fluctuations in generation, variable loads, reduced inertia, response delays, and infrastructural limitations. Therefore, it is essential to utilize appropriate controllers in the LFC structure to enhance the performance of the LFC in the presence of these resources. In Table 1 of the paper, various methods for LFC in islanded microgrids are reviewed. These methods include the Fuzzy Logic controller [11],  $H_\infty$  robust control [12–15], SMC controller [16, 17], PI-PD cascaded controller based on SSO [18], Type II fuzzy logic [19], PI-PD cascaded controller based on GWO [20], 1PD-3DOFPID controller based on COA [21], Hybrid FPD-TID controller based on CCSA [22], FOPID controller [23], MPC controller [24], CF-FOIDF Controller [25], FTID Controller based on SO [26], Robust PID Controller [27], Output Feedback Control Method based on LMI [28–30], and LADRC Controller [31]. Each of these methods employs different optimization and control techniques to enhance frequency stability and address challenges such as load variations, reduced inertia, and parameter uncertainties.

The MPC controller is a model-based control method that calculates the optimal control signal at each time step based on the current system conditions, desired reference, and existing constraints. Using the system's dynamic model, MPC predicts the future state of the system over a specified time horizon. Due to its numerous advantages, such as the ability to forecast system behavior, manage constraints, and optimize multiple variables simultaneously, the MPC is widely used in advanced control systems. However, MPC also faces certain challenges and limitations, including the following:

1. Dependence on an Accurate System Model: MPC operates based on a precise mathematical model of the system. If the system model is not correctly identified or lacks sufficient accuracy, the controller's performance may degrade. This inaccuracy can be particularly problematic in systems with complex dynamics, time variations, or uncertainties.

2. Limitations in Dealing with Disturbances and Uncertainty: It is inherently designed for controlling linear or well-modeled systems. In the presence of unknown disturbances or environmental uncertainties, its performance can weaken, as these disturbances are not accounted for in the predictive model.

3. High Computational Complexity: It typically requires solving an optimization problem at each time step. If the number of state or input variables and constraints is large, this optimization can lead to high computational complexity, causing issues in real-time applications.

4. Sensitivity to Rapid Changes in System Parameters: It operates under the assumption of a fixed or known model of the system. However, in microgrids, the parameters of the system can change over time or under varying conditions. These changes can result in instability or reduced performance of the MPC controller.

To address the limitations of the MPC controller, this paper employs a Feedforward neural network (FNN). In fact, FNN can provide better estimates of unknown or complex system dynamics

by learning from system data, thereby enhancing the MPC in the face of incomplete models. The FNN can also be used to estimate disturbances. By learning the behavior of disturbances from past data, the neural network can predict future disturbances and assist the MPC controller in making better decisions and mitigating the effects of these disturbances. Additionally, the FNN can learn adaptively, tracking changes in system parameters over time. Therefore, in combination with MPC, the FNN can serve as a tool for updating the system model in response to parametric changes.

In this paper, to improve the performance of the LFC against production fluctuations, variable loads, reduction of inertia, disturbances, and uncertainties related to microgrids, an MPC based on deep learning is designed. Deep learning has been used to improve the performance of the MPC against disturbances and parameter uncertainty. To compare the proposed method against disturbances and parameter uncertainty, it has been compared with several methods, including LADRC and FOPID, and the results show the superiority of the proposed method compared to other mentioned methods. The proposed method has been able to be resistant to disturbances and uncertainty of microgrid parameters, improve inertia, improve frequency stability, and reduce the effect of fluctuations on islanded microgrids. The main contributions of this paper are as follows:

- Development of an advanced load frequency control (LFC) method: In this paper, a new LFC method for islanded microgrids is proposed that uses model predictive control (MPC) enhanced with deep learning techniques. This approach addresses the challenges posed by distributed generation (DGs) and electric vehicles (EVs).

- Integration of deep learning with MPC: In this paper, a feedforward neural network (FNN) is also designed with the MPC framework to improve the controller performance against uncertainties and disturbances. The FNN learns from historical data to predict disturbances and adaptively update the system model, increasing the robustness of the MPC controller.

- Superior performance in disturbance rejection: The MPC based on FNN method shows superior performance in disturbance rejection compared to traditional control methods such as linear active disturbance rejection controllers (LADRC) and fractional order proportional integral derivative controllers (FOPID). The results indicate improved frequency stability and better handling of oscillations in the microgrid.

- Comprehensive validation through experiments: The simulations that have been carried out have proven the effectiveness of the proposed method (The MPC based on FNN) against disturbances and uncertainties related to the parameters related to the islanded microgrid.

The paper consists of several Sections. In the Section 2, the islanded microgrid structure is discussed. In the Section 3, the design of the proposed controller is discussed to improve the performance of the LFC loop. In the Section 4, the simulation of the suggested technique and its comparison with other methods used in the field of LFC are discussed. In the Section 5, the conclusion is stated.

## 2. THE MICROGRID UNDER STUDY

### 2.1. Structure of the islanded microgrid

In an islanded microgrid, like the power system, the balance between production and consumption must be maintained by the LFC system, the presence of DGs and EVs due to production fluctuations, variable loads, reduction of inertia, disturbances, and uncertainty related to system parameters, performance It will complicate the LFC. In Fig. 1, the structure of the islanded microgrid is shown [31]. This system includes SG, FC, ESS, PV, WT, and EV. In Fig. 2, the dynamic model of the islanded microgrid considering the EV is shown. This dynamic model is a first-order model (reduced order) that is suitable for the stability analysis of the islanded microgrid [31].

Table 1. Various controllers used in the LFC system structure of islanded microgrids.

Methodologies employed	Main findings	Deficiency of the method used
Fuzzy logic controller [11]	Improved frequency stability and resistant to slight uncertainties	Not resistant to disturbances
$H_\infty$ robust control [12–15]	Improving frequency stability and being resistant to mild disturbances as well as being resistant to uncertainty	Lack of ability against severe disturbances, need to know the exact model of the system
SMC controller [16, 17]	Improving frequency stability and being resistant to mild disturbances as well as being resistant to uncertainty	Lack of ability against severe disturbances, need to know the exact model of the system
PI-PD cascaded controller based on SSO [18]	Improving frequency stability and being resistant to mild disturbances as well as being resistant to uncertainty	Lack of ability against severe disturbances
Type II Fuzzy Logic [19]	Improved frequency stability and resistant to slight uncertainties	Not being resistant to disturbances on the islanded microgrid
PI-PD cascaded controller based on GWO [20]	Improving frequency stability and being resistant to mild disturbances as well as being resistant to uncertainty	Lack of ability against severe disturbances
IPD-3DOFPID controller based on COA [21]	Improving frequency stability and being resistant to mild disturbances as well as being resistant to uncertainty	Lack of ability against severe disturbances
Hybrid FPD-TID based on CCSA [22]	Improving frequency stability and being resistant to mild disturbances as well as being resistant to uncertainty	Lack of ability against severe disturbances
FOPID controller [23]	Improved frequency stability and robustness against mild uncertainty	Not resistant to disturbances
MPC controller [24]	Improved frequency stability and robustness against mild uncertainty	Not resistant to extreme disturbances and extreme uncertainty
CF-FOIDF controller [25]	Improved frequency stability and robustness against mild uncertainty	Not resistant to extreme disturbances
FTID controller based on SO [26]	Improved frequency stability and robustness against mild uncertainty	Not resistant to extreme disturbances
Robust PID [27]	Improving frequency stability and resistant to parameter uncertainty	Not resistant to extreme disturbances
Output feedback control method based on LMI [28–30]	Improving frequency stability and being resistant to mild disturbances as well as being resistant to uncertainty	Lack of ability against severe disturbances, need to know the exact model of the system
LADRC [31]	Improving frequency stability and resistant to disturbances	Inability to deal with uncertainty related to system parameters

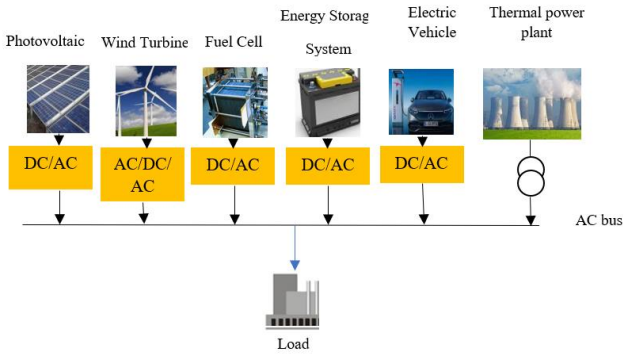


Fig. 1. The structure of the islanded microgrid [31].

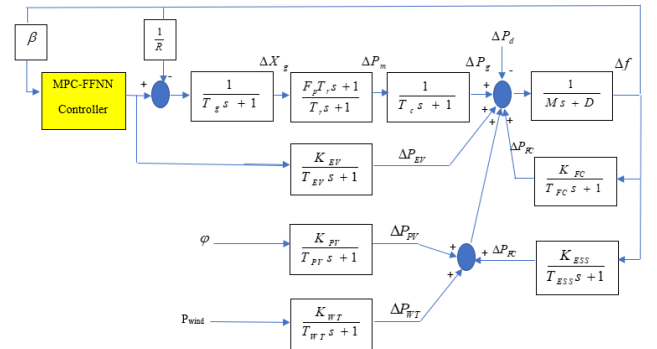


Fig. 2. The dynamic model of the islanded microgrid considering the EV [31].

## 2.2. The state-space equations related to the islanded microgrid

Eq. (1) displays the state-space equations of a system. Eq. (2) display the microgrid state-space equations. Table 2 displays the parameters pertaining to the islanded microgrid [31].

$$\begin{aligned} \dot{x}(t) &= Ax(t) + Bu(t) + Dw(t) \\ y(t) &= Cx(t) \end{aligned} \quad (1)$$

## 3. THE SUGGESTED TECHNIQUE TO RAISE THE LFC'S PERFORMANCE

### 3.1. MPC

MPC is an advanced control method that optimizes a cost function over a forecast horizon using a model of the system. In MPC, a system model typically defined as a state model or a continuous-time or discrete-time linear model is used to predict the future behavior of the system based on the current values of states and inputs. This prediction occurs within a specific timeframe

Table 2. The parameters pertaining to the islanded microgrid [31].

Parameter	Value	Parameter	Value
$T_{FC}$	0.1	$D$	1
$K_{FC}$	1	$R$	1.11
$T_{ESS}$	0.1	$K_b$	40
$K_{ESS}$	1.5	$M$	8.8
$T_{PV}$	1.85	$K_{EV}$	1
$K_{PV}$	1	$T_c$	0.3
$T_{WT}$	1.5	$F_P$	1.6
$K_{WT}$	1	$T_g$	0.2
$T_{EV}$	0.1	$T_r$	12

known as the "Prediction Horizon" [32]. By defining a cost function, MPC aims to determine the best inputs for the system to ensure that its output reaches the desired value. This cost function generally accounts for the difference between predicted outputs and reference values, as well as a penalty for changes in inputs [33]. In this controller, after solving the optimization problem at each step, only the first optimal input is applied to the system, and the optimization is then performed again for subsequent steps, a process referred to as "continuous" or "receding horizon control" [34]. MPC controller, the system model is often expressed as Eq. (3):

$$\begin{aligned}
 A = & \begin{bmatrix} \frac{-D}{M} & \frac{-1}{M} & 0 & 0 & \frac{1}{M} & \frac{1}{M} & \frac{1}{M} & \frac{1}{M} & \frac{1}{M} \\ 0 & \frac{1}{T_c} & \frac{1}{T_c} & 0 & 0 & 0 & 0 & 0 & 0 \\ \frac{-F_P}{RT_g} & 0 & \frac{-1}{T_r} & \frac{T_g - F_P T_r}{T_r T_g} & 0 & 0 & 0 & 0 & 0 \\ \frac{-1}{RT_g} & 0 & 0 & \frac{-1}{T_g} & 0 & 0 & 0 & 0 & 0 \\ 0 & 0 & 0 & 0 & \frac{-1}{T_{EV}} & 0 & 0 & 0 & 0 \\ \frac{K_{FC}}{T_{FC}} & 0 & 0 & 0 & 0 & \frac{-1}{T_{FC}} & 0 & 0 & 0 \\ \frac{K_{ESS}}{T_{ESS}} & 0 & 0 & 0 & 0 & 0 & \frac{-1}{T_{ESS}} & 0 & 0 \\ 0 & 0 & 0 & 0 & 0 & 0 & 0 & \frac{-1}{T_{PV}} & 0 \\ 0 & 0 & 0 & 0 & 0 & 0 & 0 & 0 & \frac{-1}{T_{WT}} \end{bmatrix} \begin{bmatrix} \Delta f \\ \Delta X_g \\ \Delta P_m \\ \Delta P_g \\ \Delta P_{EV} \\ \Delta P_{FC} \\ \Delta P_{ESS} \\ \Delta P_{PV} \\ \Delta P_{WT} \end{bmatrix} + \\
 & \begin{bmatrix} 0 \\ 0 \\ \frac{F_P}{T_g} \\ \frac{1}{T_r} \\ \frac{K_{EV}}{T_{EV}} \\ 0 \\ 0 \\ 0 \\ 0 \end{bmatrix} [u] + \begin{bmatrix} \frac{-1}{M} \\ 0 \\ 0 \\ 0 \\ 0 \\ 0 \\ 0 \\ 0 \\ 0 \end{bmatrix} w(t) \\
 y(t) = & [\beta \ 0 \ 0 \ 0 \ 0 \ 0 \ 0 \ 0 \ 0] \begin{bmatrix} \Delta f \\ \Delta X_g \\ \Delta P_m \\ \Delta P_g \\ \Delta P_{EV} \\ \Delta P_{FC} \\ \Delta P_{ESS} \\ \Delta P_{PV} \\ \Delta P_{WT} \end{bmatrix}
 \end{aligned} \quad (2)$$

$$\begin{aligned}
 x(k+1) &= Ax(k) + Bu(k) \\
 y(k) &= Cx(k) + Du(k)
 \end{aligned} \quad (3)$$

$x(k)$  represents the system's states at time (k) in Eq. (3) [35]. The control input at time (k) is denoted by  $u(k)$ . When the system is at time (k), its output is  $y(k)$ . Here are the state model matrices (A), (B), (C), and (D).

The cost function used in MPC for optimization is shown as Eq. (4).

$$\begin{aligned}
 J = & \sum_{i=0}^{N-1} ((y(k+i|k) - r(k+i))^T Q (y(k+i|k) - \\
 & r(k+i)) + \Delta u(k+i)^T R_1 \Delta u(k+i)
 \end{aligned} \quad (4)$$

The expected output at time (k+i) in Eq. (4) is  $y(k+i|k)$ , which is dependent on data at time (k). The reference value, or set point at time (k+i), is denoted by  $r(k+i)$ . The change in control input is denoted by  $u(k+i)$ . The weighting matrix for the output error is denoted by  $Q$ .  $R_1$  is the weighting matrix for control inputs.  $N$  represents the forecast range.

In order to maintain smooth and steady control, this cost function penalizes significant changes in the inputs while attempting to minimize the difference between the anticipated outputs and the reference values. One of the important advantages of MPC is the ability to impose constraints. These constraints can include constraints on inputs, outputs, or even system states. For example, in Eq. (5), the limit on the input signal is shown [33].

$$u_{\min} < u(k) < u_{\max} \quad (5)$$

These limits make the inputs or outputs of the system not exceed certain values, which is very critical in microgrids (frequency control). At each instant of time, the MPC controller solves an optimization problem. This problem includes the minimization of the cost function with respect to system constraints and control constraints [34]. The result of this optimization is a sequence of inputs for the prediction horizon. From this sequence, only the first value is applied to the system [34].

MPC is inherently designed for controlling linear or well-modeled systems. However, in an islanded microgrid, its performance can be compromised by unknown disturbances or uncertainties related to system parameters, as these factors are often not included in the predictive model. Additionally, MPC typically requires solving an optimization problem at each moment. In islanded microgrids, the large number of state variables, inputs, and constraints can lead to high computational complexity, making real-time applications challenging. To address these limitations of the MPC controller in islanded microgrids, this paper employs FNN. FNN can effectively estimate unknown or complex system dynamics by learning from system data, thereby enhancing the performance of MPC in the presence of imperfect models. Furthermore, FNN can estimate disturbances by analyzing past data to predict future disturbances, enabling the MPC controller to make more informed decisions and mitigate the impact of these disturbances. Additionally, FNN has the capability to learn adaptively, allowing it to adjust to changes in system parameters over time.

### 3.2. FNN

FNN is one of the types of neural networks used to solve the problems of sequence processing and temporal data [36]. These networks are able to preserve past state and use it in future times, which allows them to maintain long-term relationships and model temporal dependencies [37].

In Fig. 3, an example of a FNN is shown [38]. This type of network is structured as an acyclic directed graph, meaning there are no feedback loops or recurring connections [39]. Three different kinds of layers make up this system: input, hidden, and output layers [39]. The input layer is the first layer and is responsible for receiving and processing data or features before they enter the network [40]. The output layer, on the other hand, delivers the network's results or predictions, with its activation function varying based on the specific problem being addressed [40]. In an FNN, a series of functions are applied to the input

data, and using multiple hidden layers allows for the computation of complex functions by breaking them down into simpler steps. In general, FNNs can contain multiple hidden layers. Each neuron within these layers acts as a processing unit within the network [40].

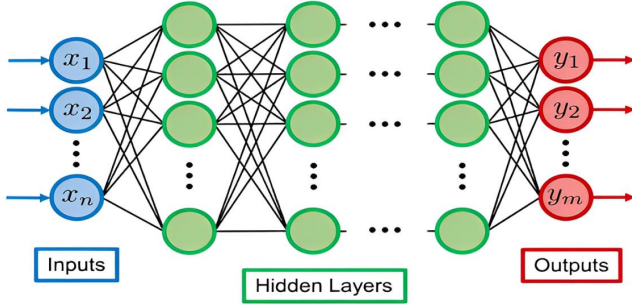


Fig. 3. The FNN [38].

The neural network neuron is depicted in Fig. 4 as a two-step process that involves computing the weighted sum of the inputs and applying an activation function to normalize the result [40].

In this neuron,  $x_1$  to  $x_n$  are equivalent to the inputs,  $W_1$  to  $W_n$  are equivalent to the corresponding weights, and  $b$  represents the bias, and the  $f$  function is applied to the weighted sum of the inputs. Actuator functions can be linear or non-linear [40]. In a neuron's output, the activator function serves as a decision-making hub. Based on the activation functions, a neuron learns either linear or non-linear decision limits [40]. Also, this function normalizes the output of the neurons to prevent the output of the neuron from becoming too large after several layers. For each input of a neuron, there are corresponding weights. During the training phase, the network has to learn these parameters [40].

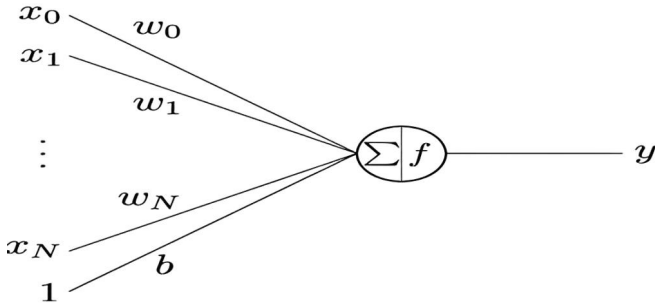


Fig. 4. The diagram of neural network neurons [40].

The network is given training examples, and the output that is produced is compared to the intended output. The error generated by this comparison is employed to iteratively adjust the weights of the neurons, gradually minimizing the overall error. This weight adjustment process is accomplished through the utilization of the backpropagation algorithm [40].

### 3.3. The training algorithm

The Levenberg-Marquardt algorithm is specifically designed for solving nonlinear optimization problems and training FNN. This algorithm combines two optimization methods: gradient descent and Newton's method. Below are the key steps and equations of this algorithm:

1. Objective of the algorithm:

Eq. (6) defines the cost function  $J(\theta)$ , and the algorithm's objective is to reduce it.

$$J(\theta) = \frac{1}{2} \sum_{i=1}^m (y_i - \hat{y}_i)^2 \quad (6)$$

$Y_i$  represents the real output in Eq. (6). Where  $m$  is the number of samples and  $\hat{y}_i$  is the models projected output.

2. Gradient calculation:

Eq. (7) defines the gradient of the cost function in regard from the factors (weights and biases).

$$\nabla J(\theta) = \frac{\partial J(\theta)}{\partial \theta} \quad (7)$$

3. Hessian calculation

Eq. (8) defines the Hessian matrix, which holds the second derivatives of the cost function.

$$H = \frac{\partial^2 J(\theta)}{\partial \theta^2} \quad (8)$$

4. Update rule

The parameter update in the Levenberg-Marquardt algorithm is defined in Eq. (9).

$$\theta_{new} = \theta_{old} - (J^T J + \lambda I)^{-1} J^T r \quad (9)$$

In Eq. (9),  $\theta$  represents the parameters (weights and biases). The initial derivatives of the cost function with dignity to the parameters are represented by the Jacobian matrix  $J$ .  $r$  is the residual vector defined as  $r = y - \hat{y}$  is a damping factor that helps control the update behavior.  $I$  is the identity matrix.

Table 3. The pseudo-code of MPC controller design based on FNN.

#### Pseudo-code:

##### Initialize parameters:

$T_s = 0.05$ ;  $N = 10$ ;  $n_x = 9$ ;  $n_u = 1$ ;  $n_{neurons} = 20$ ;  $T = 50$ ;  
 $A_{nominal}, B, C, D = \text{define\_state\_space\_matrices}()$ ;

##### Define Neural Network (NN):

$net = \text{create\_feedforward\_neural\_network}(n_{neurons}, n_{layers})$ ;  
 Set NN training parameters: epochs, learning rate, etc.

##### Generate training data:

$(X_{train}, Y_{train}) = \text{generate\_synthetic\_data}(n_x, n_u, \text{uncertainty})$ ;  
 Train the NN using  $X_{train}$  and  $Y_{train}$ ;

##### Define MPC controller:

$mpcObj = \text{create\_MPC\_controller}(A_{nominal}, B, C, D, T_s, N)$ ;  
 Set MPC cost function weights:  $Q, R$ ;  
 Define control input constraints;

##### Simulation Loop (for each timestep $k$ ):

for  $k = 1$  to  $num\_steps$ :

Simulate parameter uncertainty:

$uncertainty = \text{generate\_random\_uncertainty}(n_x)$ ;

$A_{modified} = A_{nominal} + uncertainty$ ;

Predict disturbances using NN:

$last\_u = \text{get\_last\_control\_input}(u\_history, k)$ ;

$input\_to\_nn = \text{concatenate}(x, last\_u, uncertainty)$ ;

$disturbance = \text{NN\_predict}(net, input\_to\_nn)$ ;

Update state-space model with disturbance:

$A_{updated} = A_{modified} + disturbance$ ;

$update\_MPC\_model(mpcObj, A_{updated}, B, C, D)$ ;

Compute control action using MPC:

$u = \text{MPC\_compute\_control\_action}(mpcObj, x, r)$ ;

Update system state:

$x = A_{nominal} \cdot x + B \cdot u$ ;

Save results:

$x\_history[k] = x$ ;

$u\_history[k] = u$ ;

Plot results;

5. Damping factor adjustment

Table 4. Input and output parameters related to FNN.

FNN outputs	FNN inputs
$\Delta f$	$d_1$
$\Delta X_g$	$d_2$
$\Delta P_m$	$d_3$
$\Delta P_g$	$d_4$
$\Delta P_{EV}$	$d_5$
$\Delta P_{FC}$	$d_6$
$\Delta P_{ESS}$	$d_7$
$\Delta P_{PV}$	$d_8$
$\Delta P_{WT}$	$d_9$
$u$	
$\Delta P_d$	
$\Delta M$	
$\Delta D$	
$\Delta R$	
$\Delta T_g$	
$\Delta T_r$	
$\Delta F_P$	
$\Delta K_{FC}$	
$\Delta K_{ESS}$	

Table 5. MPC and FNN controller parameters.

Parameters related to FNN		Parameters related to the MPC controller	
N	10	neurons	20
$T_S$	0.05	epochs	200
Q	diag[10 1 1 1 1 1 1 1]	Number of training data samples	5000
$R_1$	0.1	Number of hidden layers	4
$u(k)$	[-0.5 0.5]	Learning rate	0.01

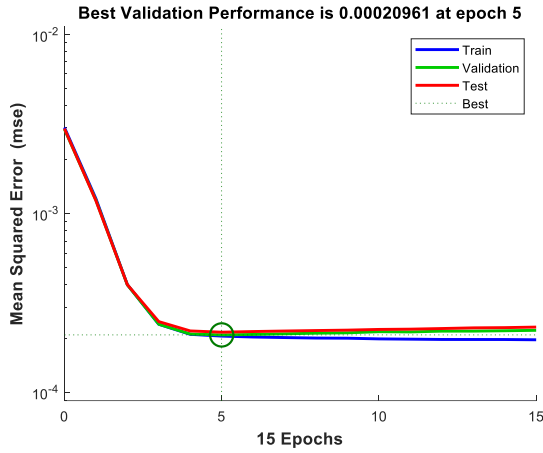


Fig. 5. The performance diagram of FNN training.

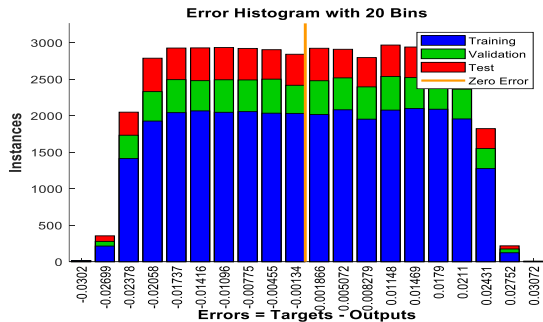


Fig. 6. The error histogram.

The damping factor  $\lambda$  is adjusted dynamically:

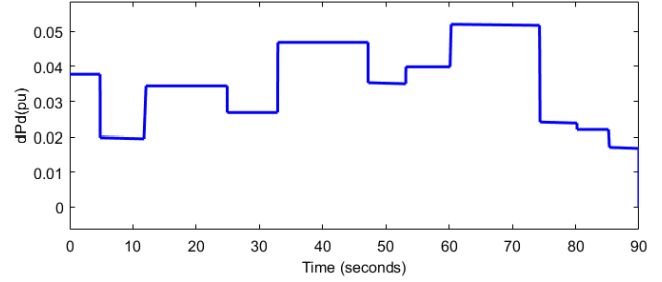


Fig. 7. A small disruption is first applied to the islanded microgrid.

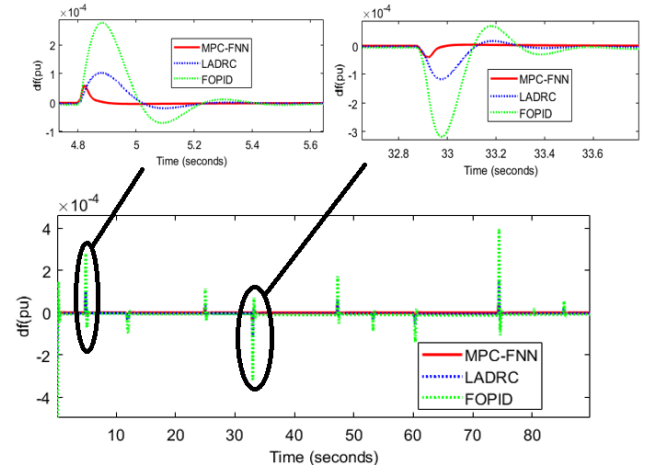


Fig. 8. The FR of the islanded microgrid using different controllers, Scenario (1).

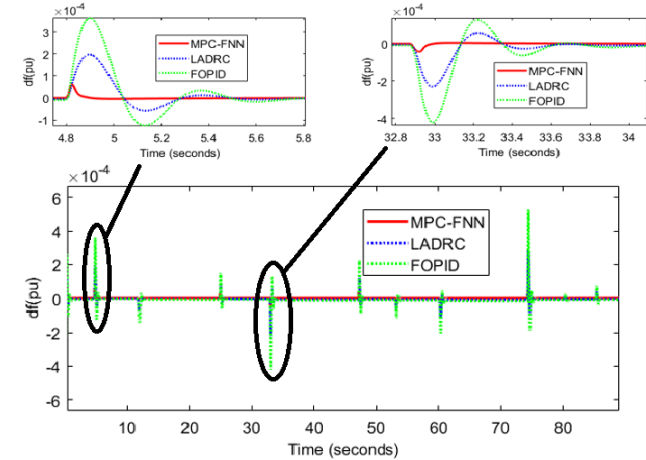


Fig. 9. The FR of the islanded microgrid using different controllers, Scenario (2).

If the update results in a decrease in the cost,  $\lambda$  is decreased (moving toward Newton's method). If the cost increases,  $\lambda$  is increased (moving toward gradient descent).

### 6. Convergence check

Until the cost function change is less than a predetermined threshold or the maximum number of iterations is achieved, these procedures are repeated.

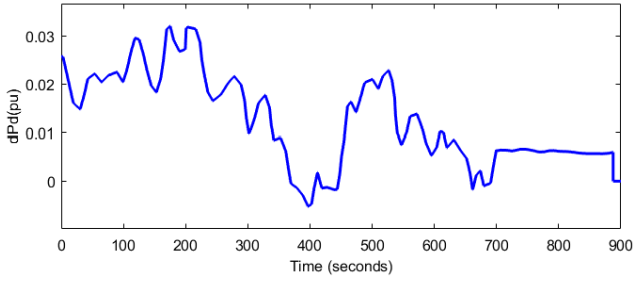


Fig. 10. The islanded microgrid is initially subjected to a significant disruption, Scenario (3).

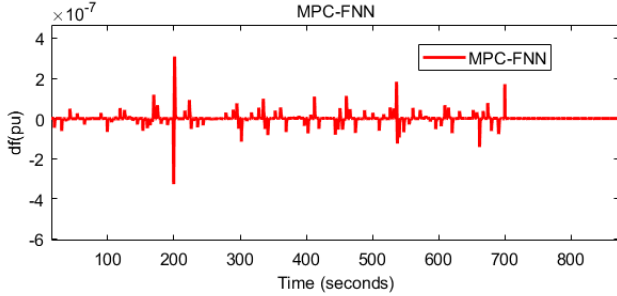


Fig. 11. The FR of the islanded microgrid using MPC-FNN controllers, Scenario (3).

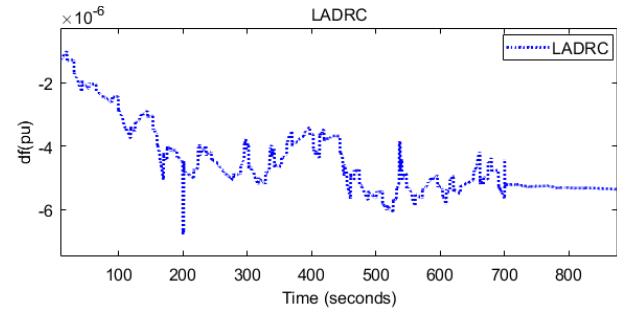


Fig. 12. The FR of the islanded microgrid using the LADRC controller, Scenario (3).

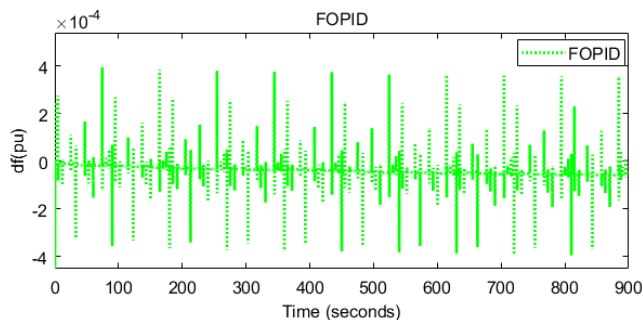


Fig. 13. The FR of the islanded microgrid using the FOPID controller, Scenario (3).

### 3.4. Designing of the MPC based on FNN to improve LFC performance in islanded microgrid

In this paper, FNN acts as a compensator against parameter uncertainty and disturbances on the island microgrid along with the MPC controller. In particular, the role of FNN in MPC controller

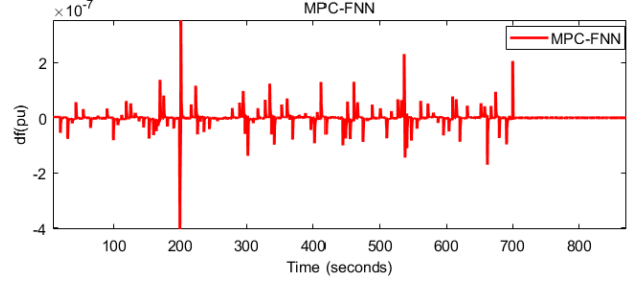


Fig. 14. The FR of the islanded microgrid using MPC-FNN controllers, Scenario (4).

denominator can be divided into several parts:

1) Prediction of disturbances and uncertainties: FNN is designed to predict disturbances and uncertainties in islanded microgrid parameters. These random changes such as uncertainty in the matrix (A) can negatively affect the performance of the islanded microgrid. FNN predicts these disturbances and uncertainties using its inputs (including system states, control input, and parameter uncertainties). In fact, by predicting these disturbances and uncertainties, FNN helps to modify the system model in the MPC controller and, as a result, obtain better control in the presence of uncertainties and disturbances.

2) Compensation of disturbances and parametric uncertainties: After predicting disturbances and parametric uncertainties by FNN, this information is used in the system model to modify the matrix (A). By updating the system model based on these predictions, the MPC controller can make better control decisions and compensate for existing disturbances and uncertainties. In other words, FNN helps the MPC make more optimal decisions because the MPC now has an updated and more realistic model of the system. It has the power to include more accurate predictions of perturbations and parameter changes.

3) Ability to adapt to parameter changes: FNN can perform well in situations where the system undergoes unexpected parameter changes due to its ability to adapt to changes. This allows the system to remain stable in the face of various and unforeseen changes.

In general, the role of FNN in this paper is to predict and compensate for parameter uncertainties and disturbances on the island microgrid, which helps the MPC controller to perform better in the face of uncertain conditions and provide accurate control. FNN helps improve system performance in real time by updating the system model and predicting disturbances.

The pseudo-code of MPC controller design based on FNN in order to improve LFC performance in islanded microgrid is shown in Table 3.

## 4. SIMULATION

Table 2 displays the islanded microgrid's parameters. The FNN's inputs, outputs, and structure are then described. The 19 inputs of FNN comprise the following: the present status of the islanded microgrid, the control signal produced by the MPC, and any disruptions or uncertainties pertaining to the islanded microgrid's characteristics. The outputs of FNN are the predicted disturbance values for 9 states of the islanded microgrid ( $d_1, d_2, \dots, d_9$ ). These outputs are used as input to the islanded microgrid model to compensate the dynamic changes of the system in the face of uncertainties and disturbances.

In this way, FNN uses information on system states and control input as well as disturbances to predict future disturbances and this information is used as feedback in the system model so that the MPC controller can perform better. In Table 4, the input and output parameters of FNN are shown. Levenberg-Marquardt algorithm has been used to train FNN. The parameters related to

the MPC and FNN controller are shown in Table 5. According to the information in Table 3 and Table 4, the training process related to FNN has been simulated in MATLAB software. In Fig. 5, the performance diagram of FNN training is shown, which has the best performance in iteration 5 and its value is equal to 0.00020961. In Fig. 6, the error histogram is shown. According to the graphs related to the FNN training, this method has been able to map the inputs to the outputs in the neural network.

Simulation has been done in four scenarios. Using several controllers, the impact of a little disruption on the islanded microgrid in scenario (1) has been studied. The impact of a small disruption and a small degree of uncertainty in the islanded microgrid's characteristics employing various controllers has been studied in scenario (2). Using several controllers, the impact of a major disruption on the islanded microgrid has been studied in scenario (3). Several controllers have been used to examine the impact of major disruption and severe uncertainty on islanded microgrid characteristics in scenario (4).

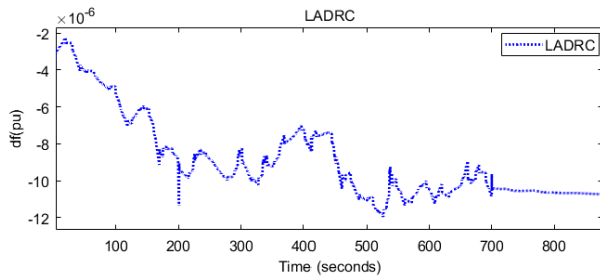


Fig. 15. The FR of the islanded microgrid using the LADRC controller, Scenario (4).

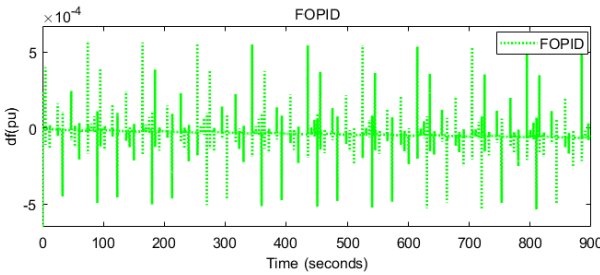


Fig. 16. The FR of the islanded microgrid using the FOPID controller, Scenario (4).

**Scenario (1):** In this scenario, a small disruption is first applied to the islanded microgrid according to Fig. 7. Fig. 8 shows the FR of the islanded microgrid using different controllers. According to the results of this scenario, the proposed method (MPC-FNN) has been able to reduce the effect of disruptions on the islanded microgrid compared to other mentioned methods, and this method has been able to reduce the frequency deviations and damp it in a faster time. Table 6 displays the outcomes of scenario (1) with various controllers. Scenario (1) evaluates the microgrid's response to a small disturbance using three controllers: MPC-FNN, LADRC, and FOPID. The results are analyzed based on their ST, MO, and MU. The analysis focuses on (ST), as well as the combined impact of MO and MU. The MPC-FNN controller achieves stabilization in  $ST = 0.4$  seconds, which is the fastest among the three controllers. The combined MO and MU values are  $0.5 \times 10^{-4}$  and  $0.3 \times 10^{-4}$ . These results demonstrate that MPC-FNN is highly effective in managing disturbances, maintaining precision and stability under challenging conditions. The LADRC controller stabilizes the system in  $ST = 1.3$  seconds, which is significantly slower than MPC-FNN. The combined MO and MU values are  $1 \times 10^{-4}$  and  $1 \times 10^{-4}$ , showing moderate overshoot and

undershoot. While LADRC performs reasonably well, its longer settling time and higher combined MO and MU values highlight its limitations in effectively handling small disturbance compared to MPC-FNN. The FOPID controller stabilizes the system in  $ST = 1.5$  seconds, making it the slowest of the three controllers. The combined MO and MU values  $3 \times 10^{-4}$  and  $3 \times 10^{-4}$ , which reflect significant overshoot and undershoot. These results indicate that FOPID struggles the most in managing small disturbances, demonstrating poor overall performance in this scenario. These results suggest that FOPID performs the weakest in this scenario, with both slow response and high deviations.

**Scenario (2):** In this case, as shown in Fig. 7, the islanded microgrid is initially subjected to a small disruption. The impact of parameter uncertainty ( $M=-30\%$ ) for the microgrid is taken into account in this scenario. The FR of the islanded microgrid with various controllers is displayed in Fig. 9. Based on the scenario findings, the suggested approach (MPC-FNN) outperforms the other approaches listed in terms of its ability to lessen the impact of disruptions on the islanded microgrid and its resilience to parameter uncertainty. Additionally, the frequency variations have been able to be dampened and reduced more quickly with the suggested strategy. Table 6 displays the outcomes of scenario (2) with various controllers. Scenario (2) evaluates the microgrid's performance under a small disturbance combined with parameter uncertainty ( $M = -30\%$ ), using three controllers: MPC-FNN, LADRC, and FOPID. The analysis focuses on (ST), as well as the combined impact of MO and MU. The MPC-FNN controller achieves stabilization in  $ST = 0.42$  seconds, which is the fastest among the three controllers. The combined MO and MU values are  $0.52 \times 10^{-4}$  and  $0.33 \times 10^{-4}$ . These results demonstrate that MPC-FNN is highly effective in managing both disturbances and parameter uncertainty, maintaining precision and stability under challenging conditions. The LADRC controller stabilizes the system in  $ST = 1.4$  seconds, which is significantly slower than MPC-FNN. The combined MO and MU values are  $2 \times 10^{-4}$  and  $2 \times 10^{-4}$ , showing moderate overshoot and undershoot. While LADRC performs reasonably well, its longer settling time and higher combined MO and MU values highlight its limitations in effectively handling parameter uncertainty compared to MPC-FNN. The FOPID controller stabilizes the system in  $ST = 1.7$  seconds, making it the slowest of the three controllers. The combined MO and MU values  $4 \times 10^{-4}$  and  $4 \times 10^{-4}$ , which reflect significant overshoot and undershoot. These results indicate that FOPID struggles the most in managing disturbances and parameter uncertainty, demonstrating poor overall performance in this scenario.

**Scenario (3):** In this case, as shown in Fig. 10, the islanded microgrid is initially subjected to a significant disruption. Using MPC-FNN controllers, the FR of the islanded microgrid is displayed in Fig. 11. The FR of the islanded microgrid using the LADRC controller is displayed in Fig. 12. The FR of the islanded microgrid using the FOPID controller is seen in Fig. 13. The outcome of this scenario indicates that, in comparison to the other ways described, the suggested approach (MPC-FNN) has been able to lessen the impact of severe disruptions on the islanded microgrid. Table 6 displays the outcomes of scenario (3) with various controllers. Scenario (3) evaluates the microgrid's response to a major disturbance using three controllers: MPC-FNN, LADRC, and FOPID. The results are analyzed based on their MO and MU. The combined MO and MU values are  $3 \times 10^{-7}$  and  $3 \times 10^{-7}$  (MPC-FNN controller). These results demonstrate that MPC-FNN is highly effective in managing disturbances, maintaining precision and stability under challenging conditions. The combined MO and MU values are  $6 \times 10^{-6}$  and  $6 \times 10^{-6}$ , showing moderate overshoot and undershoot (LADRC controller). While LADRC performs reasonably well, its higher combined MO and MU values highlight its limitations in effectively handling major disturbance compared to MPC-FNN. The combined MO

Table 6. The results of different scenarios using MPC-FNN, LADRC and FOPID controllers.

Controller	Scenario (1)			Scenario (2)			Scenario (3)			Scenario (4)		
	MO (pu)	MU (pu)	ST (sec)	MO (pu)	MU (pu)	ST (sec)	MO (pu)	MU (pu)	ST (sec)	MO (pu)	MU (pu)	ST (sec)
MPC-FNN	$0.5 \times 10^{-4}$	$0.3 \times 10^{-4}$	0.4	$0.52 \times 10^{-4}$	$0.33 \times 10^{-4}$	0.42	$3 \times 10^{-7}$	$3 \times 10^{-7}$	-	$4 \times 10^{-7}$	$4 \times 10^{-7}$	-
LADRC	$1 \times 10^{-4}$	$1 \times 10^{-4}$	1.3	$2 \times 10^{-4}$	$2 \times 10^{-4}$	1.4	$6 \times 10^{-6}$	$6 \times 10^{-6}$	-	$12 \times 10^{-6}$	$12 \times 10^{-6}$	-
FOPID	$3 \times 10^{-4}$	$3 \times 10^{-4}$	1.5	$4 \times 10^{-4}$	$4 \times 10^{-4}$	1.7	$4 \times 10^{-4}$	$4 \times 10^{-4}$	-	$6 \times 10^{-4}$	$6 \times 10^{-4}$	-

and MU values  $4 \times 10^{-4}$  and  $4 \times 10^{-4}$ , which reflect significant overshoot and undershoot. These results indicate that FOPID struggles the most in managing major disturbances, demonstrating poor overall performance in this scenario. These results suggest that FOPID performs the weakest in this scenario, with high deviations.

**Scenario (4):** In this case, as shown in Fig. 10, the islanded microgrid is initially subjected to a significant disruption. Severe uncertainty is taken into account in the islanded microgrid's parameters in this scenario (M=-30%, D=-10%, R=20%). Using MPC-FNN controllers, the FR of the islanded microgrid is seen in Fig. 14. The FR of the islanded microgrid using the LADRC controller is displayed in Fig. 15. The FR of the islanded microgrid using the FOPID controller is displayed in Fig. 16. The outcome of this scenario indicates that, in comparison to the other ways discussed, the suggested approach (MPC controller based on FNN) has been able to lessen the impact of severe disruptions on the islanded microgrid. It must also be resilient to high levels of uncertainty in the microgrid's parameters. Table 6 displays the outcomes of scenario (4) with various controllers. Scenario (4) evaluates the microgrid's performance under a major disturbance combined with severe parameter uncertainty (M=-30%, D=-10%, R=20%) using three controllers: MPC-FNN, LADRC, and FOPID. The results are analyzed based on their MO and MU. The combined MO and MU values are  $4 \times 10^{-7}$  and  $4 \times 10^{-7}$  (MPC-FNN controller). These results demonstrate that MPC-FNN is highly effective in managing major disturbances and severe parameter uncertainty, maintaining precision and stability under challenging conditions. The combined MO and MU values are  $12 \times 10^{-6}$  and  $12 \times 10^{-6}$ , showing moderate overshoot and undershoot (LADRC controller). While LADRC performs reasonably well, its higher combined MO and MU values highlight its limitations in effectively handling major disturbance and severe parameter uncertainty compared to MPC-FNN. The combined MO and MU values  $6 \times 10^{-4}$  and  $6 \times 10^{-4}$ , which reflect significant overshoot and undershoot. These results indicate that FOPID struggles the most in managing major disturbances and severe parameter uncertainty, demonstrating poor overall performance in this scenario. These results suggest that FOPID performs the weakest in this scenario, with high deviations.

## 5. CONCLUSION

In the context of islanded microgrids incorporating distributed generators (DGs) and electric vehicles (EVs), load frequency control (LFC) faces increased complexities due to low inertia and fluctuations in generation. The uncertainty in the islanded microgrid's parameters, along with external disturbances, further complicates LFC performance. To address these challenges, this paper presents a model predictive control (MPC) approach enhanced by deep learning. Deep learning techniques are employed to bolster the MPC's resilience to disturbances and parameter uncertainties. The performance of the proposed method is evaluated against several benchmarks, including linear active disturbance rejection control (LADRC) and fractional-order proportional-integral-derivative (FOPID) controllers. The proposed method (MPC-FNN) improves maximum frequency deviations by 58% compared to the mentioned control methods, while the settling time of frequency deviations in the islanded microgrid improves by 66%.

## REFERENCES

- [1] N. Kumar and D. Jain, "Development of an adaptive protection scheme for microgrid operation suitable for grid-connected and islanded mode," *J. Oper. Autom. Power Eng.*, vol. 13, no. 4, pp. 255–268, 2025.
- [2] H. Shayeghi and A. Rahnama, "Frequency regulation of a standalone interconnected ac microgrid using innovative multistage tdf (1+ fopi) controller," *J. Oper. Autom. Power Eng.*, vol. 12, no. 2, pp. 121–133, 2024.
- [3] F. Jabari, M. Zeraati, M. Sheibani, and H. Arasteh, "Robust self-scheduling of pvs-wind-diesel power generation units in a standalone microgrid under uncertain electricity prices," *J. Oper. Autom. Power Eng.*, vol. 12, no. 2, pp. 152–162, 2024.
- [4] A. Khorshidi, T. Niknam, and B. Bahmani, "Synchronization of microgrid considering the dynamics of v2gs using an optimized fractional order controller-based scheme," *J. Oper. Autom. Power Eng.*, vol. 9, no. 1, pp. 11–22, 2021.
- [5] F. Amiri and M. Moradi, "Improvement of frequency stability in the power system considering wind turbine and time delay," *J. Renew. Energy Environ.*, vol. 10, no. 1, pp. 9–18, 2023.
- [6] M. Shahbazi and F. Amiri, "Designing a neuro-fuzzy controller with crps and rlse algorithms to control voltage and frequency in an isolated microgrid," in *Int. Power Syst. Conf.*, pp. 588–594, IEEE, 2019.
- [7] P. Kesavan, U. Subramaniam, D. Almakhlles, and S. Selvam, "Modeling and coordinated control of grid-connected photovoltaic, wind turbine-driven pmsg, and energy storage device for a hybrid dc/ac microgrid," *Prot. Control Mod. Power Syst.*, vol. 9, no. 1, p. 154, 2024.
- [8] A. Pamidimukkala, S. Kermanshachi, J. Rosenberger, and G. Hladik, "Barriers and motivators to the adoption of electric vehicles: A global review," *Green Energy Intell. Transp.*, 2024.
- [9] F. Amiri, M. Moradi, and M. Eskandari, "Suppression of low-frequency oscillations in hybrid/multi microgrid systems with an improved model predictive controller," *IET Renew. Power Gener.*, 2024.
- [10] F. Amiri and A. Hatami, "Load frequency control for two-area hybrid microgrids using model predictive control optimized by grey wolf-pattern search algorithm," *Soft Comput.*, vol. 27, no. 23, pp. 18227–18243, 2023.
- [11] S. Aziz, H. Wang, Y. Liu, J. Peng, and H. Jiang, "Variable universe fuzzy logic-based hybrid lfc control with real-time implementation," *IEEE Access*, vol. 7, pp. 25535–25546, 2019.
- [12] C. Peng, J. Zhang, and H. Yan, "Adaptive event-triggering h load frequency control for network-based power systems," *IEEE Trans. Ind. Electron.*, vol. 65, no. 2, pp. 1685–1694, 2017.
- [13] H. Bevrani, M. Feizi, and S. Ataee, "Robust frequency control in an islanded microgrid:  $H_\infty$  and  $\mu$ -synthesis approaches," *IEEE Trans. Smart Grid*, vol. 7, no. 2, pp. 706–713, 2015.
- [14] S. Wen, X. Yu, Z. Zeng, and J. Wang, "Event-triggering load frequency control for multiarea power systems with communication delays," *IEEE Trans. Ind. Electron.*, vol. 63, no. 2, pp. 1308–1317, 2015.
- [15] N. Chuang, "Robust load-frequency control in interconnected power systems," *IET Control Theory Appl.*, vol. 10, no. 1, pp. 67–75, 2016.

- [16] M. Sarkar, A. Dev, P. Asthana, and D. Narzary, "Chattering-free robust adaptive integral higher-order sliding mode control for load frequency problems in multi-area power systems," *IET Control Theory Appl.*, vol. 12, no. 9, pp. 1216–1227, 2018.
- [17] H. Li, X. Wang, and J. Xiao, "Adaptive event-triggered load frequency control for interconnected microgrids by observer-based sliding mode control," *IEEE Access*, vol. 7, pp. 68271–68280, 2019.
- [18] B. Khokhar, S. Dahiya, and K. Singh Parmar, "A robust cascade controller for load frequency control of a standalone microgrid incorporating electric vehicles," *Electr. Power Compon. Syst.*, vol. 48, no. 6-7, pp. 711–726, 2020.
- [19] M. Khooban, T. Niknam, F. Blaabjerg, P. Davari, and T. Dragicevic, "A robust adaptive load frequency control for microgrids," *ISA Trans.*, vol. 65, pp. 220–229, 2016.
- [20] S. Padhy, S. Panda, and S. Mahapatra, "A modified gwo technique-based cascade pi-pd controller for agc of power systems in the presence of plug-in electric vehicles," *Eng. Sci. Technol. Int. J.*, vol. 20, no. 2, pp. 427–442, 2017.
- [21] I. Davoudkhani, P. Zare, A. Abdelaziz, M. Bajaj, and M. Tuka, "Robust load-frequency control of islanded urban microgrid using 1pd-3dof-pid controller including mobile ev energy storage," *Sci. Rep.*, vol. 14, no. 1, p. 13962, 2024.
- [22] B. Khokhar, S. Dahiya, and K. Parmar, "A novel hybrid fuzzy pd-tid controller for load frequency control of a standalone microgrid," *Arab. J. Sci. Eng.*, vol. 46, pp. 1053–1065, 2021.
- [23] S. Debbarma and A. Dutta, "Utilizing electric vehicles for lfc in restructured power systems using fractional order controller," *IEEE Trans. Smart Grid*, vol. 8, no. 6, pp. 2554–2564, 2017.
- [24] F. Banis, D. Guericke, H. Madsen, and N. Poulsen, "Load-frequency control in microgrids using target-adjusted mpc," *IET Renew. Power Gener.*, vol. 14, no. 1, pp. 118–124, 2020.
- [25] Y. Arya, "Effect of electric vehicles on load frequency control in interconnected thermal and hydrothermal power systems utilizing cf-foidf controller," *IET Gener. Transm. Distrib.*, vol. 14, no. 14, pp. 2666–2675, 2020.
- [26] A. Rai and D. Das, "The development of a fuzzy tilt integral derivative controller based on the sailfish optimizer to solve load frequency control in a microgrid, incorporating energy storage systems," *J. Energy Storage*, vol. 48, p. 103887, 2022.
- [27] R. Sadiq, Z. Wang, C. Chung, D. Gan, and C. Tong, "Coordinated robust pid-based damping control of permanent magnet synchronous generators for low-frequency oscillations considering power system operational uncertainties," *J. Mod. Power Syst. Clean Energy*, 2023.
- [28] F. Amiri and M. Moradi, "Design of a new control method for dynamic control of the two-area microgrid," *Soft Comput.*, vol. 27, no. 10, pp. 6727–6747, 2023.
- [29] F. Amiri and M. Moradi, "Coordinated control of lfc and smes in the power system using a new robust controller," *Iran. J. Electr. Electron. Eng.*, vol. 17, no. 4, p. 1912, 2021.
- [30] F. Amiri and M. Moradi, "Designing a new robust control for virtual inertia control in the microgrid with regard to virtual damping," *J. Electr. Comput. Eng. Innov.*, vol. 8, no. 1, pp. 53–70, 2020.
- [31] P. Sharma and S. Neeli, "Computation of stability boundary locus of robust pid controller for time delayed lfc system," *Int. J. Dyn. Control*, vol. 12, no. 5, pp. 1455–1465, 2024.
- [32] F. Amiri, M. Eskandari, and M. Moradi, "Virtual inertia control in autonomous microgrids via a cascaded controller for battery energy storage optimized by firefly algorithm and a comparison study with ga, pso, abc, and gwo," *Energies*, vol. 16, no. 6611, 2023.
- [33] F. Amiri and M. Moradi, "A new control strategy for controlling isolated microgrid," *Energy Eng. Manage.*, vol. 10, no. 4, pp. 60–73, 2023.
- [34] A. Aydinoglu, A. Wei, W. Huang, and M. Posa, "Consensus complementarity control for multi-contact mpc," *IEEE Trans. Robot.*, 2024.
- [35] L. Jin, L. Liu, X. Wang, M. Shang, and F. Wang, "Physical-informed neural network for mpc-based trajectory tracking of vehicles with noise considered," *IEEE Trans. Intell. Veh.*, 2024.
- [36] B. Yang, B. Liang, Y. Qian, R. Zheng, S. Su, Z. Guo, and L. Jiang, "Parameter identification of pemfc via feedforward neural network-pelican optimization algorithm," *Appl. Energy*, vol. 361, p. 122857, 2024.
- [37] K. Wong, R. Dornberger, and T. Hanne, "An analysis of weight initialization methods in connection with different activation functions for feedforward neural networks," *Evol. Intell.*, vol. 17, no. 3, pp. 2081–2089, 2024.
- [38] M. Admon, N. Senu, A. Ahmadian, Z. Majid, and S. Salahshour, "A new modern scheme for solving fractal-fractional differential equations based on deep feedforward neural network with multiple hidden layers," *Math. Comput. Simul.*, vol. 218, pp. 311–333, 2024.
- [39] M. Al-Zamzami, A. Al-Gheethi, S. Alzaeemi, M. Al-Sahari, M. Al-Maqtari, and E. Noman, "Validity of zinc oxide nanoparticles biosynthesized in food wastes extract in treating real samples of printing ink wastewater; prediction models using feed-forward neural network (fnn)," *Chemosphere*, vol. 362, p. 142793, 2024.
- [40] X. Guo, W. Wang, J. Zhang, and L. Gong, "An online growing-and-pruning algorithm of a feedforward neural network for nonlinear systems modeling," *IEEE Trans. Autom. Sci. Eng.*, 2024.